Cancer Therapy: Preclinical

Clinical Cancer Research

Development and Characterization of HPV-Positive and HPV-Negative Head and Neck Squamous Cell Carcinoma Tumorgrafts

Randall J. Kimple[1,6], Paul M. Harari[1,6], Alexandra D. Torres[1,2], Robert Z. Yang[1,2], Benjamin J. Soriano[3], Menggang Yu[4,6], Eric A. Armstrong[1], Grace C. Blitzer[1], Molly A. Smith[1], Laurel D. Lorenz[2], Denis Lee[2], David T. Yang[3,6], Timothy M. McCulloch[5,6], Gregory K. Hartig[5,6], and Paul F. Lambert[2,6]

Abstract

Purpose: To develop a clinically relevant model system to study head and neck squamous cell carcinoma (HNSCC), we have established and characterized a direct-from-patient tumorgraft model of human papillomavirus (HPV)–positive and HPV-negative cancers.

Experimental Design: Patients with newly diagnosed or recurrent HNSCC were consented for donation of tumor specimens. Surgically obtained tissue was implanted subcutaneously into immunodeficient mice. During subsequent passages, both formalin-fixed/paraffin-embedded as well as flash-frozen tissues were harvested. Tumors were analyzed for a variety of relevant tumor markers. Tumor growth rates and response to radiation, cisplatin, or cetuximab were assessed and early passage cell strains were developed for rapid testing of drug sensitivity.

Results: Tumorgrafts have been established in 22 of 26 patients to date. Significant diversity in tumorgraft tumor differentiation was observed with good agreement in degree of differentiation between patient tumor and tumorgraft (Kappa 0.72). Six tumorgrafts were HPV-positive on the basis of p16 staining. A strong inverse correlation between tumorgraft p16 and p53 or Rb was identified (Spearman correlations $P = 0.085$ and $P = 0.002$, respectively). Significant growth inhibition of representative tumorgrafts was shown with cisplatin, cetuximab, or radiation treatment delivered over a two-week period. Early passage cell strains showed high consistency in response to cancer therapy between tumorgraft and cell strain.

Conclusions: We have established a robust human tumorgraft model system for investigating HPV-positive and HPV-negative HNSCC. These tumorgrafts show strong correlation with the original tumor specimens and provide a powerful resource for investigating mechanisms of therapeutic response as well as preclinical testing. *Clin Cancer Res; 19(4); 855–64. ©2012 AACR.*

Introduction

Head and neck squamous cell carcinoma (HNSCC) is the sixth most common worldwide cancer with approximately 620,000 new diagnoses annually (1). The development of these cancers has been traditionally associated with tobacco and alcohol use. Evidence in recent years has identified an etiologic role of human papillomavirus (HPV) in a substantial subset of patients with HNSCC, many of whom do not have a strong history of tobacco and alcohol use (2).

Radiation alone or with concurrent chemotherapy is an important component of therapy for patients with HNSCC. Treatment can be quite toxic with significant acute and long-term side effects. Retrospective and prospective analyses confirm a striking difference in clinical outcome between HPV-positive and HPV-negative HNSCC (3). However, at present, there is no compelling data that therapy recommendations can be guided on the basis of HPV status. To facilitate the development of novel therapy approaches and to better understand molecular mechanisms that underlie therapeutic responses, robust preclinical model systems are needed.

We sought to establish and validate a direct-from-patient human tumorgraft model system of HNSCC that could be utilized to identify molecular targets, validate novel therapeutics, guide treatment recommendations, and facilitate studies regarding biologic mechanisms of treatment sensitivity and/or resistance. Such tumorgraft model systems differ from traditional xenograft model

Authors' Affiliations: [1]Department of Human Oncology; [2]McArdle Laboratory for Cancer Research and Department of Oncology; [3]Department of Pathology; [4]Department of Biostatistics and Medical Informatics; [5]Department of Surgery, Otolaryngology; [6]University of Wisconsin Carbone Cancer Center, University of Wisconsin, Madison, Wisconsin

Note: Supplementary data for this article are available at Clinical Cancer Research Online (http://clincancerres.aacrjournals.org/).

Corresponding Author: Randall J. Kimple, Department of Human Oncology, University of Wisconsin Comprehensive Cancer Center, 3107 WIMR, 1111 Highland Avenue, Madison, WI 53705. Phone: 608-265-9156; Fax: 608-263-9947;
E-mail: rkimple@humonc.wisc.edu

doi: 10.1158/1078-0432.CCR-12-2746

Translational Relevance

We describe and characterize a direct-from-patient tumorgraft model system of human head and neck cancer including tumors derived from both human papillomavirus–associated cancers and tobacco-associated cancers. Comparisons of primary tumor and tumorgrafts in addition to the significant diversity of tumor morphology suggest that this resource represents an outstanding platform for investigating novel therapeutics and combinations of chemotherapy and/or radiation. These tumorgrafts may prove to be a valuable resource for optimizing therapy for specific subgroups of patients with head and neck cancer and may shed light into the molecular mechanisms underlying differential therapeutic responses between HPV-positive and HPV-negative head and neck cancer.

systems in that the human tumors are grafted directly from human subjects into immunodeficient mice, rather than first being established as cell lines in tissue culture and then being engrafted onto mice. The biologic relevance of the traditional cell line-based xenograft model system has come under increased scrutiny at various levels including recent system wide analyses suggesting that immortalized cell lines from a variety of tumor types retain greater gene expression similarity to each other than to their tissue of origin (4, 5). The tumorgraft model system is increasingly recognized as a preclinical model system that may provide greater biologic relevance to human cancers at many levels including tumor pathology, growth, metastasis, disease outcome, and drug responsiveness (6–8).

Materials and Methods

Patient selection

Patients with newly diagnosed or recurrent HNSCC were approached for possible tissue donation. Patients consenting to participate in this IRB-approved protocol completed a brief questionnaire collecting information regarding tobacco use, alcohol use, prior malignancy, sex, age, and prior treatment received. At the time of surgery or staging biopsy, a section of tumor was collected for research use making sure not to compromise surgical margin or pathologic assessment.

Mice

Immunodeficient mice used for tumorgraft development included male and female NOD scid gamma (NSG, Jackson Laboratories) and Hsd:athymic Nude-*Foxn1*^{nu} (Harlan Laboratories). All mice were kept in the Association for Assessment and Accreditation of Laboratory Animal Care approved Wisconsin Institute for Medical Research Animal Care Facility and studies with them were carried out in accordance with an approved animal protocol.

Establishment of tumorgrafts

Tumor was transported directly from the operating room to the laboratory in ice-cold culture media [Dulbecco's Modified Eagle Medium (DMEM) with 10% fetal bovine serum (FBS), 1% penicillin/streptomycin, and 25 μg/mL amphotericin] and minced in a culture dish to less than 1 mm^3 pieces under sterile conditions. Minced tumor pieces were mixed 1:1 with reduced growth factor Matrigel (cat #354230, BD Biosciences, Inc) and injected subcutaneously into NSG mice with an 18 gauge needle as passage zero (P0). Every effort was made to accomplish this transfer within 1 hour of tumor harvest from the surgical procedure. Subsequent passages were made in a similar fashion into either NSG or athymic nude mice.

Cryopreservation of tumorgrafts was accomplished by mixing minced tumor pieces with transport media supplemented with 10% dimethylsulfoxide (DMSO). Tumors were frozen in controlled rate freezers (1°C/minute) to −80°C overnight and transferred to liquid nitrogen for long-term storage. To thaw tumors, aliquots were warmed to 37°C in a heated water bath and tumor tissue was washed twice in transport media (without DMSO) and immediately implanted into mice.

Histology of primary and tumorgrafts

At each passage, a section of the tumor was reserved for fixation in 10% neutral-buffered formalin and subsequent embedding in paraffin blocks. Five-μm sections were cut and hematoxylin and eosin (H&E) stains were conducted on every 10th section. Each patient's primary tumor was also stained by H&E and slides imaged on an Olympus BX51 microscope (Olympus America, Inc). Comparisons between primary tumor, first passage tumorgraft, and subsequent tumorgraft passages were made by a surgical pathologist on the basis of differentiation, keratinization, and overall tumor architecture.

Assessment of human papillomavirus

Early passage (P0–P2) tissue at the time of harvest from immunodeficient mice was snap frozen in liquid nitrogen. Total genomic DNA and total RNA from this tissue were isolated using the DNeasy Blood and Tissue Kit, the miRNeasy Mini Kit, and RNeasy minElute spin column (Cat#69504, 217004, and 74204, respectively, from Qiagen Inc). Multiple methods were used to assess for the presence of HPV.

Quantitative real-time PCR (qRT-PCR) was carried out on a BioRad CFX96. Briefly, total RNA was harvested using the miRNeasy with the MinElute Kit with snap-frozen tissue samples from passage 0. cDNA was synthesized using the iScript Reverse Transcription Supermix Kit (Bio-Rad Laboratories) and 1,000 ng of total RNA. qRT-PCR was carried out by using IQ Multiplex Powermix with 10 ng cDNA per 10 μL reaction. *GAPDH*, *HPV-16 E5*, *E6*, and *E7* transcripts were detected using primers and probes (Supplementary Table S1) purchased from Integrated DNA Technologies, Inc. The thermocycler was programmed for an initial 95°C for 7 minutes followed

by 40 cycles of 94°C for 15 seconds and 60°C for 30 seconds.

Total genomic DNA was used to probe for HPV DNA using a nested PCR approach previously described (9). Briefly, for both rounds of PCR, a final concentration of 1× PCR buffer, 0.2 mmol/L dNTPs, 1.5 mmol/L $MgCl_2$, and 0.2 U Taq was used. In the first round, 100 ng of purified DNA and MY09 and MY11 (Supplementary Table S1) primers (which detect multiple HPV subtypes) at 0.2 μmol/L were used. The thermocycler was programmed for an initial 94°C for 4 minutes followed by 40 cycles of 94°C for 15 seconds, 55°C for 30 seconds, and 72°C for 1 minute with final extension at 72°C for 5 minutes. Final products from PCR reactions were run on a 1.5% agarose gel, stained with ethidium bromide, and imaged.

Southern blot was conducted using 10 μg of BamHI digested total cellular DNA separated on a 1.25% agarose gel, transferred to Hybond N+ nylon membrane (Amersham) and crosslinked. DNA probes were made by 5′ end labeling 10 pmoles of HPV16-specific oligonucleotides (Supplementary Table S1) in the presence of T4 polynucleotide kinase (New England Biolabs Inc) with [γ-^{32}P] ATP (6,000 Ci/mmol) at 37°C for 1.5 hours. The membrane was prehybridized with Church hybridization buffer for 15 minutes at 52°C followed by probe hybridization for 18 hours at 52°C in a hybridization oven. Membrane was washed with Church wash buffer, exposed to a storage phosphor screen and scanned using a Typhoon 8610 imaging system (Amersham).

To assess for alternative HPV subtypes, an additional PCR for the *HPV E1* gene was carried out. Briefly, 100 ng of total genomic DNA was amplified using the degenerate *E1* primers (Supplementary Table S1) with the thermocycler programmed for an initial 94°C for 5 minutes followed by 40 cycles of 95°C for 10 seconds, 50°C for 10 seconds, and 72°C for 30 seconds with final extension at 72°C for 5 minutes. Final products were run on a 1.5% agarose gel, stained with ethidium bromide, and imaged. Positive bands were individually gel purified and sent for Sanger sequencing using the *E1* primers. Sequences were annealed, base discrepancies edited, and the resulting ideal sequence compared via BLAST search.

Radiation and chemotherapy growth delay

Tumor growth rates and therapeutic response were monitored by injecting athymic nude mice subcutaneously ($n =$ 12 per group) with tumors into bilateral flanks. Tumor volume was monitored twice weekly by measurement with Vernier calipers and calculated according to the equation $V = (\pi)/6 \times$ (large diameter) $\times$ (small diameter)^2. When individual tumor volumes reached 200 mm^3, mice were stratified into treatment groups based on tumor size such that each group had tumors with a similar range in size as determined by Wilcoxon rank-sum test. Treatment commenced the next day with cisplatin (2 mg/kg), cetuximab (0.2 mg), or vehicle control (0.95 normal saline) delivered by intraperitoneal (IP) injection twice weekly. Radiation (2 Gy/fraction twice weekly) was delivered via an X-RAD 320 biologic irradiator (Precision X-Ray) using custom-designed mouse jigs to immobilize animals and limit radiation exposure to the tumors on the dorsal flanks. Time to tumor quadrupling was calculated from the first day of treatment. Curves were fit to an exponential growth equation and compared using the extra-sum-of-squares f test using Graphpad Prism v 5.0d.

Immunohistochemistry

The expression of p16 (BD Pharmingen catalog #550834), p53, Rb, and EGFR was detected in histologic sections of tumorgrafts by standard immunohistochemistry (IHC). A one-step Gomori's trichrome stain (ENG Scientific) was used to develop 5 μ paraffin sections of passage 0 tumorgrafts. Briefly, sections were deparaffinized, incubated in Bouins solution for 1 hour at 60°C, washed in running tap water, and the nuclei stained with Weigert's iron hematoxylin for 15 minutes. Next, the slides were placed in Gomori's trichrome stain and incubated 20 minutes at room temperature. Finally, the tumor sections were rinsed with H_20, dehydrated, cleared, and coverslipped.

Images were acquired with a 20× objective using an Olympus BX51 fluorescent microscope and photographed with a SPOT RT CCD camera (Diagnostic Instruments, Inc.). A determination of positive versus negative was made by a board certified pathologist based on cytoplasmic and/or nuclear positivity more than 2+ intensity in more than 70% of tumor cells (10). The intensity of p53 and Rb staining was scored as follows: negative when less than 5% of tumor cells displayed staining; 1+ when intensity was mild; 2+, moderate; 3+, when intensity was equal to the positive control; and 4+ when intensity was greater than the positive control (11).

Results

Establishment of tumorgrafts

A total of 37 patients with head and neck cancer have been consented for tumor collection and establishment as tumorgrafts. Twenty-six had tumor collected and implanted subcutaneously into NSG mice as described in the Methods. The remaining 9 patients did not undergo tumor collection for the study because of limitations in tumor quantity, the altered timing of surgery, and/or the availability of laboratory personnel for immediate tissue transfer. Average age of donors was 61 (range 45–87). To date, 22 samples have given rise to viable tumors (take rate: 85%). Molecular characterization and assessment of HPV infection was carried out for all tumors. Comprehensive tumor growth rate assessment and therapeutic evaluation have been carried out for 3 tumorgraft models to date: UW-SCC6, UW-SCC14N, and UW-SCC22.

Clinical characteristics of the 26 patients who had tumor collected and the relationship to tumor take rate are presented in Table 1. Briefly, by univariate analysis patient sex, tobacco use, alcohol use, and T-stage did not correlate with tumorgraft take rate. Successful tumorgraft take was also not correlated with primary tumor differentiation or HPV status. However, tumorgraft establishment was significantly

Table 1. Clinical characteristics of patients and corresponding frequency of tumorgraft establishment by variable

Patient and tumor characteristics				
Parameter	**Variable**	**Patients (*n*)**	**Tumor take rate (%)**	**Significance[a]**
Age	<60	13	85	NS
	≥60	13	85	
Sex	Male	18	83	NS
	Female	8	88	
Tobacco use	Nonsmoker	7	100	NS
	Minimal use (<20 pack years)	1	100	
	>Minimal use	18	78	
Alcohol use	None/light	9	100	NS
	Moderate	6	83	
	Heavy	11	73	
T stage	T1 or T2	12	83	NS
	T3 or T4	14	86	
Nodal status	Node negative	11	64	$P = 0.02$
	Node positive	15	100	
Differentiation	Well	11	82	NS
	Moderate	11	82	
	Poor	4	100	
HPV status	Positive	8	100	NS
	Negative	13	100	
	Testing not done	*5*	*20*	

[a]The frequency of tumor take compared via Fisher's exact test (age, sex, T-stage, nodal status, and HPV status) or Chi-squared test (tobacco use, alcohol use, differentiation).

higher (100% vs. 64%, $P = 0.02$) from subjects with lymph node metastases than from those without lymph node metastases, regardless of whether the tumor biopsy was taken from the primary tumor site or from a metastatic lymph node.

Tumorgraft comparison with primary tumors

As shown in Table 2, tumorgrafts were established from multiple subsites of the head and neck including oropharynx (base of tongue and tonsil), oral cavity, and hypopharynx. The 22 successful tumorgrafts analyzed were composed of poorly differentiated tumor histology in 5 cases, moderately differentiated in 9 cases, and well differentiated in 8 cases. Figure 1 shows representative images from 3 tumorgrafts including H&E stain and p16 IHC of both the primary tumor and early passage tumorgraft, trichrome stain, and IHC of biomarkers p53, Rb, and EGFR. Strong retention of overall tumor histology including cell morphology, stromal component architecture, and the presence of cystic structures were observed between original patient tumor and tumorgraft (Fig. 1) and in sections from multiple serial passages of the same tumorgraft (Fig. 2A). In addition, good agreement with regard to the degree of tumor differentiation (i.e., poor, moderate, or well) was observed between patient specimen and tumorgraft (Fig. 2B, unweighted Kappa 0.72). To date, 17 tumors that were established in mice (P0 generation) have been successfully passaged with growth evident in the subsequent (i.e., P1) generation. Of those tumors that have been passaged at least once ($n = 22$), the mean time from initial tumorgraft implantation to first passage was 115 days and to second passage ($n = 17$) was 109 days (Fig. 2C, $P = 0.55$). Eight tumors have been passaged at least 4 times. Comparisons of differentiation over multiple passages in a single tumorgraft have shown remarkable stability (Supplementary Table S2) with a probability of change of differentiation estimated at 3% (one-sided 95% CI: 15.8%).

Cryopreservation of tumorgrafts

One challenge of utilizing direct from patient tumorgrafts is that tumor characteristics may change over time. While we have not seen this to date, we have attempted to cryopreserve tumorgrafts to allow us to reanimate early passage tumors at later time points. To date, 16 tumorgrafts have been cryopreserved and 10 have been thawed and reimplanted into NSG mice. At this time, 6 of 10 (60%) have successfully grown additional tumor.

Assessment of HPV

In light of the causal association and prognostic significance of HPV infection in head and neck cancer, we assessed the HPV status of all tumorgrafts. HPV status was

Table 2. Immunohistochemical characteristics and HPV status of tumorgraft at early passage

Tumorgraft	Tumor site	Differentiation of primary	Differentiation of tumorgraft	p53[a]	Rb[b]	Primary tumor p16 status (% of cells > = 2+ for p16)	Tumorgraft p16 status (% of cells > = 2+ for p16)	*HPV-16 E6/E7* qRT-PCR[c]	MY9/11[d]	Southern blot[d]	Degenerate *E1* PCR[d]	HPV subtype from *E1* sequencing[d]
UW-SCC1P	Base of Tongue	Moderate	Moderate	++	++	positive (70%)	positive (80%)	+	+	+	+	16
UW-SCC3P	Tonsil	Poor	Poor	+	+++	positive (95%)	negative (30%)	−	−	−	−	
UW-SCC4P	Floor of Mouth	Well	Well	+	+	positive (70%)	positive (70%)	+	+	+	+	16
UW-SCC6P	Tonsil	Moderate	Moderate	+	+	positive (90%)	positive (90%)	+	+	+	+	16
UW-SCC10P	Oral Tongue	Moderate	Poor	++	+++	negative (0%)	negative (30%)	−	−	−	−	
UW-SCC12P	Base of Tongue	Well	Well	+++	++	positive (90%)	negative (30%)	−	−	−	−	
UW-SCC13P	Oral Tongue	Well	Well	+++	+++	negative (0%)	negative (10%)	−	−	−	−	
UW-SCC14N	Base of Tongue	Moderate	Moderate	+	−	positive (90%)	negative (0%)	−	−	−	−	
UW-SCC15P	Floor of Mouth	Poor	Poor	++	++	negative (5%)	negative (0%)	−	+	−	+	16
UW-SCC17P	Tonsil	Poor	Poor	+	+	positive (95%)	positive (95%)	+	+	+	+	16
UW-SCC20P	Floor of Mouth	Well	Moderate	NE	NE	ND	NE	NE	NE	NE	NE	
UW-SCC22P	Floor of Mouth	Well	Well	+++	+++	negative (20%)	negative (0%)	−	−	−	−	
UW-SCC23P	Floor of Mouth	Well	Well	+++	+++	negative (10%)	negative (0%)	−	−	−	−	
UW-SCC24P	Floor of Mouth	Well	Well	+++	++	negative (0%)	negative (20%)	−	−	−	−	
UW-SCC25P	Floor of Mouth	Moderate	Moderate	+++	−	negative (10%)	positive (95%)	−	+	−	±	negative
UW-SCC30P	Floor of Mouth	Moderate	Well	+++	++	negative (0%)	negative (0%)	−	−	−	−	
UW-SCC31P	Hypopharynx	Poor	Poor	+	+++	negative (0%)	negative (0%)	−	−	−	−	
UW-SCC32P	Buccal mucosa	Well	Well	+++	++	negative (10%)	negative (10%)	−	−	−	−	
UW-SCC33P	Supraglottis	Moderate	Moderate	+++	+++	negative (40%)	negative (50%)	−	−	−	−	
UW-SCC34P	Buccal mucosa	Moderate	Moderate	+	+	negative (0%)	negative (10%)	−	−	−	−	
UW-SCC35P	Aveolar ridge	Well	Moderate	++	++	negative (10%)	negative (20%)	−	−	−	−	
UW-SCC36P	Tonsil	Moderate	Moderate	+	−	positive (90%)	positive (80%)	−	+	−	+	16

Abbreviations: ND, not done; NE, not evaluable.

[a]Correlation between p16 and Rb and between primary tumor HPV and Rb (Spearman correlation $P = 0.002$ and 0.034, respectively).

[b]Correlation between p16 and p53 and between primary tumor HPV and p53 (Spearman correlation $P = 0.085$ and 0.005, respectively).

[c]Conducted on cDNA generated from mRNA.

[d]Conducted on total genomic DNA.

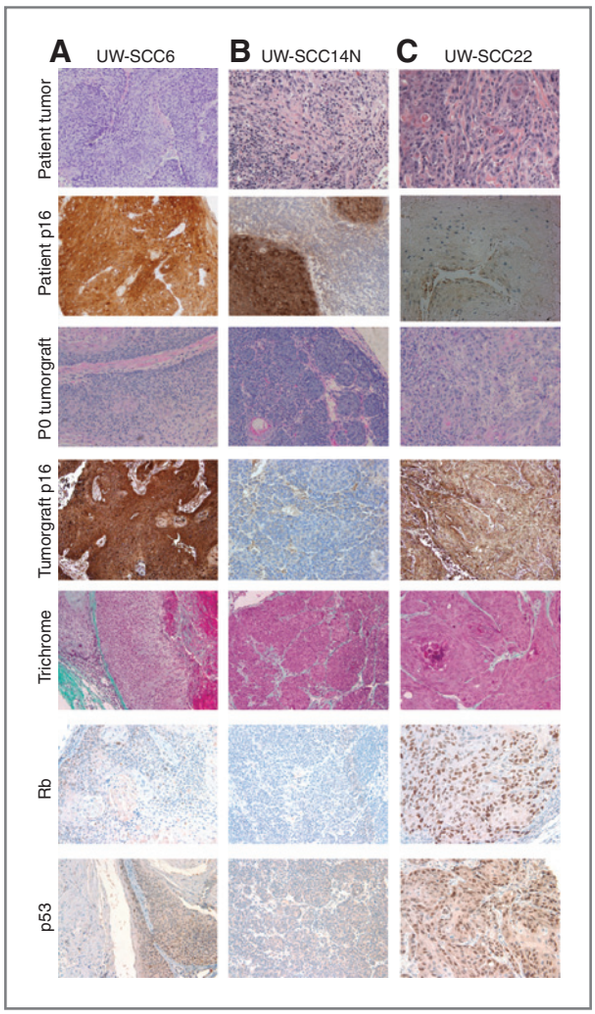

Figure 1. Histopathologic features of 3 patient tumors and corresponding tumorgrafts. UW-SCC6 (A), UW-SCC14N (B), and UW-SCC22 (C). Shown are photomicrographs of primary tumor H&E and p16 IHC top 2 rows in addition to tumorgraft passage 1 H&E, p16 IHC, Trichrome, Rb, and p53. Overall, a strong correlation between Rb and p53 staining was observed (Spearman correlation $P = 0.04$). Images at 200×.

assessed by p16 staining of the primary tumor (i.e., surgical specimen) in all but 1 patient. The primary pathologic specimens of 8 patients were HPV positive by p16 staining; 6 on the basis of at least 70% of cells having greater than equal to 2+ p16 staining, and 2 on p16 staining scored as positive versus negative at an outside institution for which slides were not available for quantification of p16 positivity (Table 2).

All tumorgrafts were assessed for HPV status using 4 distinct tests: (i) expression of p16, a surrogate marker for HPV infection, was assessed by IHC showing 6 of 22 tumorgrafts positive for p16 expression (Fig. 1); (ii) qRT-PCR for *HPV-16 E6* and *E7* RNA, showing 4 of 22 tumorgrafts positive by qRT-PCR (Table 2, Fig. 2D); (iii) PCR-based detection was used to identify the presence of HPV DNA from total genomic DNA using 2 different set of degenerate primers known to detect multiple mucosotropic HPV genotypes (9), showing 7 of 22 tumorgrafts positive by HPV-specific PCR (Table 2, Supplementary Fig. S1A); and, (iv) Southern blot of total genomic DNA for HPV-16 and HPV-18, the 2 most frequently associated papillomaviruses, was conducted using a procedure that can detect down to 0.1 copy per cell, showing 4 of 22 cases positive (Table 2, Supplementary Fig. S1B).

In addition, samples from tumorgrafts that were positive on *E1* degenerate PCR were assessed by Sanger sequencing to determine the specific HPV subtype. All showed near 100% identity with *HPV-16*. One sample, UW-SCC25P was faintly positive upon PCR with the MY9/11 primers and showed a positive doublet product by PCR using primers specific for *E1*. However, upon sequencing, these products, they showed no identity to any HPV subtype.

Differences between p16 staining of the primary surgical specimen and resultant tumorgraft were seen in 4 cases. In 3 of these cases, a different cutoff value for HPV positivity would have led to agreement between patient and tumorgraft. For example, UW-SCC3 and UW-SCC12 showed 90% of cells p16 positive in the primary and 30% of cells p16 positive in the tumorgraft. Alternatively, UW-SCC25 was scored as p16-negative in the primary (10% of cells p16 positive) and p16-positive in the tumorgraft (95% of cells p16 positive). One case, UW-SCC14N had strong p16 staining in the primary tumor, isolated cells positive for p16 in the lymph node and no p16 positive cells in the tumorgraft derived from the lymph node. Those tumors with 4 of more passages were assessed for p16 staining in each passage and showed no alteration in p16 staining over time (Supplementary Table S2).

Molecular markers—p53, Rb

Because of their known importance in HPV-associated malignancy and their central role as tumor suppressor proteins, we assessed the tumorgrafts for p53 and Rb expression by IHC. A wide range of staining for both markers was identified (Fig. 1 and Table 2) with a strong inverse correlation between p16 and p53 and between p16 and Rb detection (Spearman correlations $P = 0.03$ and $P < 0.001$, respectively) as would be expected on the basis of the mechanism of HPV oncogenesis.

Response to therapy

As an initial effort to assess the utility of tumorgrafts for therapeutic response, tumorgrafts from 3 different patients were tested in detail for response to radiation, cisplatin, and cetuximab (Fig. 3A–C). Tumorgrafts from each patient exhibited notably distinct growth patterns and response profiles to these 3 treatments. UW-SCC14N, which derived from a metastatic cervical lymph node, displayed the fastest growth rate and limited response to radiation (Table 3). In contrast, the 2 tumorgrafts derived from primary lesions, UW-SCC6 and UW-SCC22, despite very different overall growth profiles (Fig. 3), responded well to radiation, showing a 2-fold increase in time to tumor quadrupling. Both of

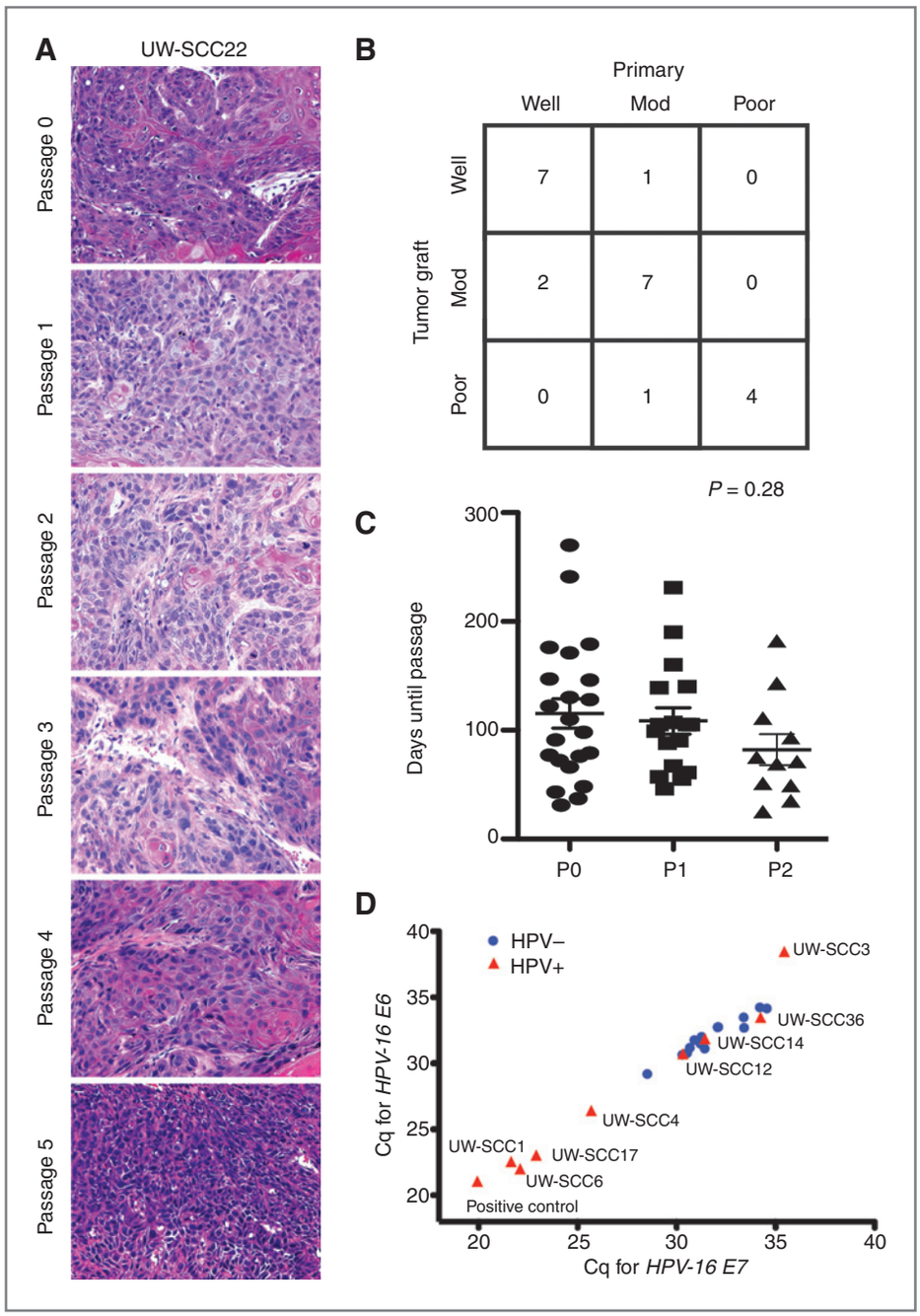

Figure 2. A, well-differentiated primary tumor along with consistency between passages. B, overall correlation between patient and tumorgraft differentiation showing good agreement (unweighted Kappa = 0.72, Std error = 0.13). C, scatterplot depicting time from implantation to passage for the initial implantation (P0) and the second (P1) and third (P2) passages. One-way ANOVA, $P = 0.28$. D, qRT-PCR with primers specific for HPV-16 E6 and HPV-16 E7 RNA show high correlation in Cq values between E6 and E7 (HPV-negative, circles; HPV+, triangles), Pearson $r = 0.96$, $P < 0.0001$.

these tumorgrafts responded more briskly to cetuximab than to cisplatin, which was not the case for UW-SCC14N.

The patient donating tissue for UW-SCC6 presented with a T2N2BM0 oropharyngeal cancer and was treated with radiation and concurrent cisplatin. The patient developed lung metastases approximately 17 months after primary treatment, but remained controlled at the site of the primary and in the neck. UW-SCC14N presented with T1N2B oropharyngeal cancer and underwent an initial neck dissection followed by radiation and concurrent cetuximab chemotherapy. The patient's disease is controlled 17 months after initial therapy. UW-SCC22 presented with a T4aN1M0 oral cavity tumor that was initially treated with surgical resection. Approximately 2 months after surgery, the tumor recurred at both the site of the primary disease and in the neck. The patient was treated with radiation and concurrent cisplatin. One year later, the patient presented with locally recurrent disease at which time the biopsy for tumorgraft was taken. The patient died several months later of progressive disease.

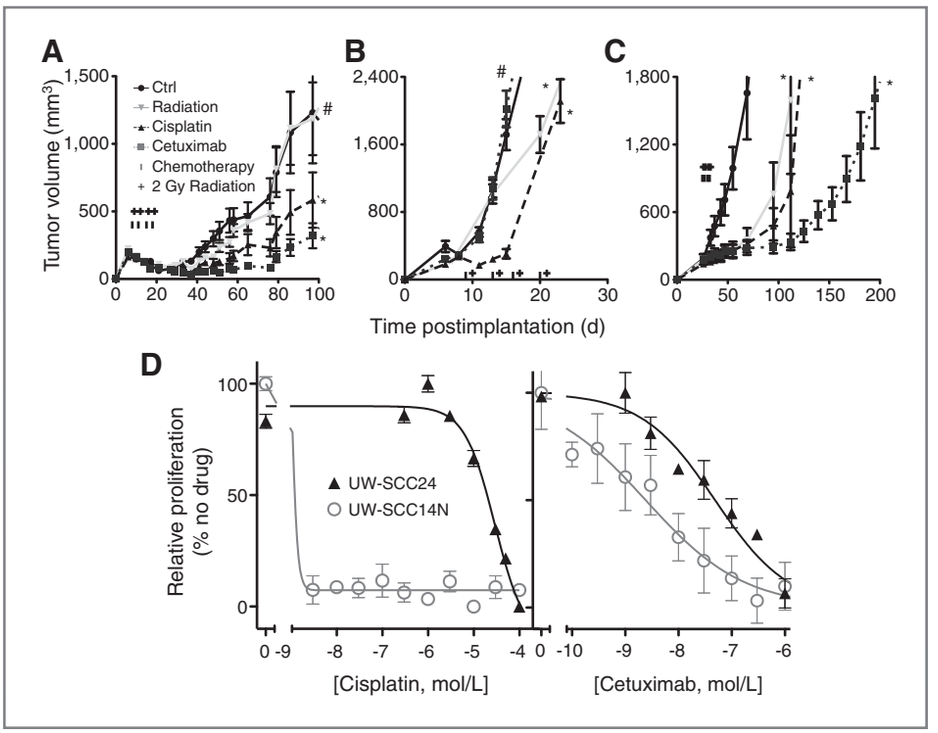

Figure 3. Effects of radiation, cetuximab, and cisplatin in 3 tumorgrafts: UW-SCC6 (A), UW-SCC14N (B), and UW-SCC22 (C). Treatments, started when subcutaneously growing tumors reached a volume of approximately 200 mm^3, were administered twice weekly for 2 weeks as described in the methods. Growth curves plotting the mean (±SEM) tumor volume over time are shown. For each group, $n = 8$–10 mice with dual tumors began treatment. *, $P < 0.01$; #, $P =$ not significant. D, early passage cell strains developed from UW-SCC24 and UW-SCC14N were assessed for proliferative potential in the presence of indicated drugs. Cell number was estimated by CCK8 assay and standardized to the maximum relative value of vehicle control.

Finally, early passage cell strains were generated directly from patient tumors if additional cells remained after the initial tumorgraft implantation, or from subsequent tumorgraft passages. To date, 6 cell strains have been generated and passaged. No difference in primary tumor characteristic seems to be predictive of cell strain development, although the power to detect such a difference is severely limited by the number of strains. The cell strains from UW-SCC14N and UW-SCC24 were tested in proliferation assays and have shown *in vitro* response to both cisplatin and cetuximab (Fig. 3D). Interestingly, a very good response to cisplatin was seen in UW-SCC14N, a tumor that also had shown a good *in vivo* response to cisplatin alone (Fig. 3B).

Table 3. Time to tumorgraft quadrupling (d) under control conditions and after radiation (2 Gy twice weekly × 4), cisplatin (0.2 mg/kg twice weekly × 4), or cetuximab (2 mg/kg twice weekly × 4)

	Ctrl	Radiation	Cisplatin	Cetuximab
UW-SCC6	44	79	91.5	123
UW-SCC14	13	13	25	17.0
UW-SCC22	55	125	125	181
% TGD (Mean ± SD)		169 ± 53	209 ± 14	247 ± 84

Abbreviation: TGD, tumor growth delay, the mean percentage increase in time to tumor quadrupling for each treatment relative to control.

Discussion

Over several decades, many investigators have relied upon tumor cell line and xenograft model systems for testing novel therapeutics. However, these systems carry significant limitations based on adaptation to growth in tissue culture including upregulation of survival genes, alterations in multidrug resistance genes, and often greater similarities to other cultured cells than to the primary tumors they were originally intended to represent (4). In addition, only 5 HPV-positive head and neck squamous cancer cell lines have been described to date (12–16), significantly limiting our ability to investigate differences between HPV-positive and HPV-negative head and neck cancers. The tumorgrafts and cell strains described in the current study represent a promising system under development by which to investigate molecular alterations underlying the growth behavior of head and neck cancers, to serve as a preclinical model system for testing novel therapeutics either alone or in combination with radiotherapy. While we would hope that this model system could someday play a useful role in the selection of optimal therapy for personalized medicine, the mean time required for tumorgraft establishment (nearly 4 months) precludes the use for initial therapeutic selection. However, Hidalgo and colleagues have successfully used tumorgrafts to identify efficacious therapies following initial therapeutic failure (7).

We commenced the current work anticipating that only a small fraction of patient tumors would grow successfully as tumorgrafts. However, the early success observed to date with 22 of 26 tumorgrafts has been highly gratifying, and may in part reflect the rapid transfer of tumor directly from patient to mouse within 1 hour, the use of matrigel to

facilitate establishment of the tumorgraft and/or the use of NSG mice, which are highly immunodeficient, as recipients. Much akin to the diverse clinical presentations of cancer patients, we have observed considerable diversity in tumor differentiation, primary site location, lymph node status, tobacco history, and HPV status (Tables 1 and 2) in the tumorgrafts. In addition, these tumorgrafts have been established from patients undergoing well-defined clinical treatments for which detailed outcome data are being carefully collected. The high tumor take rate in our study (85%) provides preliminary confidence that the process of tumorgrafting itself is not a significant selective pressure. The increased take rate of tumorgrafts from patients with lymph node metastases (regardless of the site of tissue) suggests that intrinsic factors reflecting the biology of the individual tumors may play a role in influencing tumorgraft take rates. Perhaps pooled analysis from multiple disease sites may identify critical molecular alterations associated with tumorgraft take rates.

Overall, we have observed strong histologic stability across serial passage of a single tumorgraft. While additional comparisons over multiple passages are needed to confirm phenotypic stability, our experience to date suggests high intrapatient fidelity in terms of tumor differentiation and p16 status. An exception to this pattern is the change observed in HPV-status in select patients. For example, UW-SCC14N is p16 positive in the patient's primary tumor, but negative for all tests in the tumorgraft. On the other hand, UW-SCC25 is p16 negative in the patient, but p16 positive in the tumorgraft. There are several possible explanations for these differences. It may simply reflect a difference in the percentage of cells staining p16-positive suggesting a potential selection bias in our model system. Alternatively, we and others have previously described p16-positive, HPV-negative tumors (10, 17, 18). It is unclear in our model whether the loss of p16 expression represents loss of episomal HPV-genomes, false-positive testing, alternative molecular pathway activation, or coincident tumor development. In most cases, p16 status and degenerate PCR were in agreement, those cases with discrepancies may represent false-positive results as a third test for high- and low-risk HPV using degenerate primers failed to detect a product in these cases. This seems to predominantly reflect differences in the percentage of cells staining p16-positive, thus may not represent a true difference in biology. We and others have previously described both p16-negative but *HPV*-positive cases, as well as p16-positive but *HPV* negative cancers (10, 17, 18). We did, however, identify the expected correlation between HPV-positivity and low p53 and low Rb (Table 2). Interestingly, not all groups confirm this expected correlation between HPV-positive HNC and p53 expression intensity (18–20) suggesting that there may be variation in expression of E6 and consequently incomplete p53 degradation; alternatively, mutations in p53 may be present in a subset of HPV+ HNC patients resulting in variable p53 expression.

Preclinical validation of therapeutic targets and response profiling remains an expensive and time-intensive process. There is considerable concern that human cancer cell lines, either *in vitro* or as tumor xenografts, often show limited ability to predict patient response to cancer therapy (21). This may reflect the tremendous selection pressure required to grow human tumor cells in artificial tissue culture systems with adherence to plastic ware and/or reliance on culture media. The primary tumorgraft system described in this report reflects a systematic effort to more faithfully preserve molecular, genetic, architectural, and treatment response characteristics of the original human tumor specimen. These HNSCC tumorgrafts may prove useful not only for the investigation of radiation and chemotherapy response profiles but also to uncover distinctions between HPV+ and HPV− tumors with regard to growth characteristics and response to conventional as well as new molecular therapies. Only systematic investigation over time will confirm if these tumorgraft model systems can prove consistently more faithful and predictive of true clinical response and outcome. A potential limitation of this model system is the use of immunodeficient mice necessary to enable tumorgraft growth. It has been suggested that the presence of an intact immune response in HPV+ HNC results in improved tumor control (22). However, the published data also suggest that cytotoxic therapies can result in tumor control even in the absence of an intact immune system.

An important component of the current studies is the development of cell strains. These nonimmortalized early passage cells may more faithfully represent patient response patterns; to date they show a high correlation with tumorgraft response in our hands (Fig. 3). Successful establishment of cell strains may provide a less expensive and more efficient system in which to evaluate or screen therapeutic regimens. While additional validation is necessary, our results thus far suggest that cell strains may provide a powerful adjunct to the human tumorgrafts.

In conclusion, we have described a large panel of human head and neck cancer squamous cell carcinoma tumorgrafts that reflect both HPV-positive and HPV-negative tumors. The tumorgrafts display a spectrum of differentiation typical of clinical histopathologic specimens, and a high degree of consistency between original patient tumor and tumorgraft. The combined use of early passage cell strains and tumorgrafts provides a powerful system for investigating novel therapeutics, combination therapies, and for testing hypotheses of mechanisms of therapeutic response and resistance in human head and neck cancer.

Disclosure of Potential Conflicts of Interest

No potential conflicts of interest were disclosed.

Authors' Contributions

Conception and design: R.J. Kimple, P. Harari, R.Z. Yang, P.F. Lambert
Development of methodology: R.J. Kimple, P. Harari, R.Z. Yang, E.A. Armstrong
Acquisition of data (provided animals, acquired and managed patients, provided facilities, etc.): R.J. Kimple, P. Harari, R.Z. Yang, E.A. Armstrong, G.C. Blitzer, M.A. Smith, L.D. Lorenz, D. Lee, D. Yang, T.M. McCulloch, G.K. Hartig
Analysis and interpretation of data (e.g., statistical analysis, biostatistics, computational analysis): R.J. Kimple, R.Z. Yang, B.J. Soriano, M. Yu, L.D. Lorenz, P.F. Lambert

Writing, review, and/or revision of the manuscript: R.J. Kimple, P. Harari, R.Z. Yang, L.D. Lorenz, D. Yang, T.M. McCulloch, P.F. Lambert
Administrative, technical, or material support (i.e., reporting or organizing data, constructing databases): R.J. Kimple, A.D. Torres, R.Z. Yang, M.A. Smith, D. Yang, G.K. Hartig, P.F. Lambert
Study supervision: P. Harari, P.F. Lambert

Grant Support

This study was supported by UWCCC pilot grant to P. Lambert and P. Harari and by R01 CA 113448-01(P. Harari), R01 DE017315 (P. Lambert), and U01 CA141583 (P. Lambert). R. Kimple is supported by the UW Kaye Fellowship in Head and Neck Cancer Research, K99 CA160639-01, Radiological Society of North American Research Fellow Grant, and AACR/Bristol Myers Squibb Fellowship in Clinical Cancer Research.

The costs of publication of this article were defrayed in part by the payment of page charges. This article must therefore be hereby marked *advertisement* in accordance with 18 U.S.C. Section 1734 solely to indicate this fact.

Received August 22, 2012; revised November 8, 2012; accepted November 26, 2012; published OnlineFirst December 18, 2012.

References

1. Ferlay J, Shin HR, Bray F, Forman D, Mathers C, Parkin DM. Estimates of worldwide burden of cancer in 2008: GLOBOCAN 2008. Int J Cancer 2010;127:2893–917.
2. Gillison ML, Koch WM, Capone RB, Spafford M, Westra WH, Wu L, et al. Evidence for a causal association between human papillomavirus and a subset of head and neck cancers. J Natl Cancer Inst 2000;92:709–20.
3. Lassen P. The role of Human papillomavirus in head and neck cancer and the impact on radiotherapy outcome. Radiother Oncol 2010;95:371–80.
4. Gillet JP, Calcagno AM, Varma S, Marino M, Green LJ, Vora MI, et al. Redefining the relevance of established cancer cell lines to the study of mechanisms of clinical anti-cancer drug resistance. Proc Natl Acad Sci U S A 2011;108:18708–13.
5. Uva P, Lahm A, Sbardellati A, Grigoriadis A, Tutt A, de Rinaldis E. Comparative membranome expression analysis in primary tumors and derived cell lines. PLoS One 2010;5:e11742.
6. DeRose YS, Wang G, Lin YC, Bernard PS, Buys SS, Ebbert MT, et al. Tumor grafts derived from women with breast cancer authentically reflect tumor pathology, growth, metastasis and disease outcomes. Nat Med 2011;17:1514–20.
7. Hidalgo M, Bruckheimer E, Rajeshkumar NV, Garrido-Laguna I, De Oliveira E, Rubio-Viqueira B, et al. A pilot clinical study of treatment guided by personalized tumorgrafts in patients with advanced cancer. Mol Cancer Ther 2011;10:1311–6.
8. Sivanand S, Pena-Llopis S, Zhao H, Kucejova B, Spence P, Pavia-Jimenez A, et al. A validated tumorgraft model reveals activity of dovitinib against renal cell carcinoma. Sci Transl Med 2012;4:137ra75.
9. Snijders PJ, van den Brule AJ, Schrijnemakers HF, Snow G, Meijer CJ, Walboomers JM. The use of general primers in the polymerase chain reaction permits the detection of a broad spectrum of human papillomavirus genotypes. J Gen Virol 1990;71 (Pt 1):173–81.
10. Schache AG, Liloglou T, Risk JM, Filia A, Jones TM, Sheard J, et al. Evaluation of human papilloma virus diagnostic testing in oropharyngeal squamous cell carcinoma: sensitivity, specificity, and prognostic discrimination. Clin Cancer Res 2011;17:6262–71.
11. Grant SW, Kyshtoobayeva AS, Kurosaki T, Jakowatz J, Fruehauf JP. Mutant p53 correlates with reduced expression of thrombospondin-1, increased angiogenesis, and metastatic progression in melanoma. Cancer Detect Prev 1998;22:185–94.
12. Tang AL, Hauff SJ, Owen JH, Graham MP, Czerwinski MJ, Park JJ, et al. UM-SCC-104: a new human papillomavirus-16-positive cancer stem cell-containing head and neck squamous cell carcinoma cell line. Head Neck 2012;34:1480–91.
13. Zhao M, Sano D, Pickering CR, Jasser SA, Henderson YC, Clayman GL, et al. Assembly and initial characterization of a panel of 85 genomically validated cell lines from diverse head and neck tumor sites. Clin Cancer Res 2011;17:7248–64.
14. Ferris RL, Martinez I, Sirianni N, Wang J, Lopez-Albaitero A, Gollin SM, et al. Human papillomavirus-16 associated squamous cell carcinoma of the head and neck (SCCHN): a natural disease model provides insights into viral carcinogenesis. Eur J Cancer 2005;41:807–15.
15. Gwosdz C, Balz V, Scheckenbach K, Bier H. p53, p63 and p73 expression in squamous cell carcinomas of the head and neck and their response to cisplatin exposure. Adv Otorhinolaryngol 2005;62:58–71.
16. Steenbergen RD, Hermsen MA, Walboomers JM, Joenje H, Arwert F, Meijer CJ, et al. Integrated human papillomavirus type 16 and loss of heterozygosity at 11q22 and 18q21 in an oral carcinoma and its derivative cell line. Cancer Res 1995;55:5465–71.
17. El-Naggar AK, Westra WH. p16 expression as a surrogate marker for HPV-related oropharyngeal carcinoma: a guide for interpretative relevance and consistency. Head Neck 2012;34:459–61.
18. Harris SL, Thorne LB, Seaman WT, Hayes DN, Couch ME, Kimple RJ. Association of p16(INK4a) overexpression with improved outcomes in young patients with squamous cell cancers of the oral tongue. Head Neck 2011;33:1622–7.
19. Kumar B, Cordell KG, Lee JS, Worden FP, Prince ME, Tran HH, et al. EGFR, p16, HPV Titer, Bcl-xL and p53, sex, and smoking as indicators of response to therapy and survival in oropharyngeal cancer. J Clin Oncol 2008;26:3128–37.
20. Fury MG, Drobnjak M, Sima CS, Asher M, Shah J, Lee N, et al. Tissue microarray evidence of association between p16 and phosphorylated eIF4E in tonsillar squamous cell carcinoma. Head Neck 2011;33:1340–5.
21. de Bono JS, Ashworth A. Translating cancer research into targeted therapeutics. Nature 2010;467:543–9.
22. Spanos WC, Nowicki P, Lee DW, Hoover A, Hostager B, Gupta A, et al. Immune response during therapy with cisplatin or radiation for human papillomavirus-related head and neck cancer. Arch Otolaryngol Head Neck Surg 2009;135:1137–46.